Representation of the carbon cycle in box models and GCMs 2. Organic pump

J. R. Toggweiler
Geophysical Fluid Dynamics Laboratory, NOAA, Princeton, New Jersey, USA

R. Murnane
Risk Prediction Initiative, Bermuda Biological Station for Research, Inc., Garrett Park, Maryland, USA

S. Carson and A. Gnanadesikan
Geophysical Fluid Dynamics Laboratory, NOAA, Princeton, New Jersey, USA

J. L. Sarmiento
Atmospheric and Oceanic Sciences Program, Princeton University, Princeton, New Jersey, USA

Received 27 November 2001; revised 24 July 2002; accepted 24 October 2002; published 14 March 2003.

[1] Box models of the ocean/atmosphere CO_2 system rely on mechanisms at polar outcrops to alter the strength of the ocean's organic carbon pump. GCM-based carbon system models are reportedly less sensitive to the same processes. Here we separate the carbon pumps in a three-box model and the GCM-based Princeton Ocean Biogeochemistry Model to show how the organic pumps operate in the two kinds of models. The organic pumps are found to be quite different in two respects. Deep water in the three-box model is relatively well equilibrated with respect to the pCO_2 of the atmosphere while deep water in the GCM tends to be poorly equilibrated. This makes the organic pump inherently stronger in the GCM than in the three-box model. The second difference has to do with the role of polar nutrient utilization. The organic pump in the GCM is shown to have natural upper and lower limits that are set by the initial PO_4 concentrations in the deep water formed in the North Atlantic and Southern Ocean. The strength of the organic pump can swing between these limits in response to changes in deep-water formation that alter the mix of northern and southern deep water. Thus, unlike the situation in the three-box model, the organic pump in the GCM can become weaker or stronger without changes in polar nutrient utilization. *INDEX TERMS:* 1615 Global Change: Biogeochemical processes (4805); 4267 Oceanography: General: Paleoceanography; 4806 Oceanography: Biological and Chemical: Carbon cycling; 4842 Oceanography: Biological and Chemical: Modeling; *KEYWORDS:* ocean carbon cycle, organic pump, box model, gas exchange, preformed nutrients, glacial-interglacial CO_2

Citation: Toggweiler, J. R., R. Murnane, S. Carson, A. Gnanadesikan, and J. L. Sarmiento, Representation of the carbon cycle in box models and GCMs, 2, Organic pump, *Global Biogeochem. Cycles*, *17*(1), 1027, doi:10.1029/2001GB001841, 2003.

1. Introduction

[2] The variation in atmospheric CO_2 during the Pleistocene ice ages is thought to be caused by temporal changes in the amount of organically cycled CO_2 trapped in the deep ocean (*Broecker* [1982] and many others). The mechanism that alters the organic pump remains obscure despite much effort to pin it down [*Broecker and Henderson*, 1998]. *Broecker et al.* [1999] and *Archer et al.* [2000a] have recently highlighted the fact that the mechanisms put forth in different model studies tend to be dictated by the kinds of models being used. Studies based on box models tend to focus on nutrient utilization in the Southern Ocean (for example, *Knox and McElroy* [1984], *Sarmiento and Toggweiler* [1984], and *Siegenthaler and Wenk* [1984], also known as the Harvardton Bears). Studies based on general circulation models (GCMs), on the other hand, tend to focus on mechanisms that strengthen the global fertility of the ocean [*Broecker and Henderson*, 1998; *Archer et al.*, 2000b] or increase the sinking flux of organic matter in relation to $CaCO_3$ [*Archer and Maier-Reimer*, 1994].

[3] The Southern Ocean is a region where deep water is able to come directly to the surface, take up oxygen, and release CO_2 to the atmosphere. The water that comes to the surface contains high concentrations of nitrate and phosphate. According to simple box models, the partitioning of CO_2 between the ocean and atmosphere depends on the

0886-6236/03/2001GB001841$12.00

degree to which polar organisms are able to utilize the nutrients in the upwelled deep water. Efficient nutrient utilization leads to more CO_2 retention in the deep ocean and lower atmospheric CO_2. Atmospheric CO_2 is reduced to glacial levels through a halving of polar nutrient concentrations in the three-box model of *Sarmiento and Toggweiler* [1984] and *Siegenthaler and Wenk* [1984].

[4] GCM-based carbon cycle models do not respond to polar nutrient utilization to the same extent. Complete removal of PO_4 from Southern Ocean surface waters in the Princeton carbon cycle GCM reduces atmospheric CO_2 by 71 ppm [*Sarmiento and Orr*, 1991]. This is about half the CO_2 reduction seen in the three-box model per unit nutrient reduction. There appears to be an even smaller response in the Hamburg carbon cycle GCM [*Heinze et al.*, 1991; *Archer et al.*, 2000a]. How should one interpret this difference in model behavior?

[5] *Bacastow* [1996], *Broecker et al.* [1999], and *Archer et al.* [2000a], hereinafter referred to as the Polar Skeptics, argue that the ocean's polar regions have less influence in the real ocean and in GCMs than they do in box models. They show that GCM-based carbon cycle models partition less of their CO_2 into cold deep water and relatively more CO_2 into the atmosphere and warm low-latitude surface waters. The Polar Skeptics attribute this kind of partitioning to more extensive communication between the low-latitude surface ocean and the deep ocean via vertical mixing. This vertical communication, they claim, bypasses the polar regions and renders them less important.

[6] The polar nutrient response is due to a stronger organic pump. The explanation offered by the Polar Skeptics for a weaker polar nutrient response in GCMs is based on a solubility argument. Is the Skeptics' solubility argument relevant for the organic pump, and if so, does it justify a general depreciation of polar nutrient mechanisms? The explanation for solubility differences offered by the Skeptics was shown in part 1 [*Toggweiler et al.*, 2003] to have overlooked an important fact: The solubility pump in GCMs is weaker or less efficient because GCM solutions are further from thermodynamic equilibrium. GCMs were shown, in particular, to have less CO_2 in their cold deep water because of restricted gas exchange in their polar surface waters. This finding undercuts the Skeptics' inferences about a reduced importance of the ocean's polar regions.

[7] Two themes are taken up here in part 2. The first parallels the main theme of part 1. The organic pumps in the three-box model and the GCM-based Princeton Ocean Biogeochemistry Model (POBM) are examined in isolation in order to assess the role of gas exchange. As in part 1, large differences are identified with respect to air-sea pCO_2 differences. Certainly one of the most important differences between the organic pumps in the two models is the extent of air-sea CO_2 equilibration in polar surface waters. The second theme is concerned with the polar nutrient mechanism itself. It is important to realize that the polar nutrient utilization idea came to prominence in a model that has only one polar region. The POBM, like the real ocean, has two polar regions. It becomes clear in looking at the POBM that polar nutrient depletion is not the most natural or obvious way to increase the strength of the organic pump in a system with two polar regions.

[8] Polar nutrient utilization fades in importance when once considers the different ways that deep-water forms in the ocean's two polar regions. Hence, this paper does not directly address the weak polar nutrient response seen in GCMs [e.g., *Heinze et al.*, 1991; *Archer et al.*, 2000a]. We speculate at the end of the paper that much of the weaker response is due to poor air-sea CO_2 equilibration in the deep water that forms in the Southern Ocean.

2. Organic Pump in the Three-Box Model

[9] A simple method for separating the carbon pumps in ocean models was described in part 1. The method for isolating the organic pump is briefly reviewed here. The solubility pump is first neutralized by setting the temperatures in the two surface boxes to the same value, in this case 10°C. The organic pump is then separated from the carbonate pump by setting the carbonate fraction in the sinking flux to zero. The carbonate pump can also be separated from the organic pump by setting the organic fraction in the sinking flux to zero. As in part 1, our metric for the strength of the separated pumps is the difference in total CO_2 (TCO_2) between the deep box and low-latitude surface box. Model solutions for the separated pumps are normalized to have the same atmospheric pCO_2 (280 ppm).

[10] The full method was applied in part 1 to the three-box model of *Sarmiento and Toggweiler* [1984] and *Siegenthaler and Wenk* [1984]. Pertinent details including the biological factors used to drive the model's organic and carbonate pumps are given in part 1.

[11] Table 1 repeats the solutions given in part 1 for the solubility-only, organic-only, and carbonate-only versions of the three-box model with normal (1x) and fast (30x) gas exchange. Much of the focus here is on the partial pressure of CO_2 in the polar box, pCO_{2h}, and its relationship to the partial pressures of CO_2 in the atmosphere and low-latitude box, pCO_{2atm} and pCO_{2l}, respectively. The production and remineralization of organic particles forces pCO_{2h} up in relation to pCO_{2l} and pCO_{2atm} (column 5) and drives a transfer of CO_2 from the polar box to the low-latitude box via the atmosphere. The pCO_2 differences in the carbonate-only model (column 7) are relatively small because both alkalinity and CO_2 are transported between the surface and deep boxes in $CaCO_3$ particles. This cotransport minimizes the role of air-sea transfers in the carbonate pump.

[12] Figure 1 gives results from five different configurations of the organic-only model to be discussed below. Results in the top two panels in Figure 1 are taken from columns 5 and 6 of Table 1. PO_4 concentrations (in μmol/kg) are shown on the left. TCO_2 concentrations (same units) are shown within each box on the right. The pCO_2 (in 10^{-6} atm) in each surface box is given just above along with the atmospheric pCO_2. The strength of the organic pump, $TCO_{2d} - TCO_{2l}$, is given on the far right.

[13] The polar box in the three-box model dominates the organic pump because it controls the contact between the atmosphere and the large volume of water in the deep box. The extent of this contact is mediated through PO_{4h}, the

Table 1. Surface to Deep TCO_2 Differences in the Three-Box Model

		Full Model		Solubility-Only		Organic-Only		Carbonate-Only	
Model Variable	Units	Standard Gas Exchange	30x Gas Exchange	Standard Gas Exchange	30x Gas Exchange	Standard Gas Exchange	30x Gas Exchange	Standard Gas Exchange	30x Gas Exchange
PO_{4l}	μmol/kg	0.		2.090		0.		0.	
PO_{4h}	μmol/kg	1.485		2.090		1.485		1.485	
PO_{4d}	μmol/kg	2.146		2.090		2.146		2.146	
Alk_l	μeq/kg	2266.5		2371.0		2371.0		2266.5	
Alk_h	μeq/kg	2340.8		2371.0		2371.0		2340.8	
Alk_d	μeq/kg	2373.8		2371.0		2371.0		2373.8	
TCO_{2l}	μmol/kg	1925.9	1926.5	2016.6	2009.7	2110.6	2115.4	2027.6	2027.4
TCO_{2h}	μmol/kg	2150.7	2148.8	2157.7	2174.4	2141.3	2116.7	2087.9	2090.0
TCO_{2d}	μmol/kg	2258.1	2256.2	2157.7	2174.4	2227.2	2202.6	2109.4	2111.5
pCO_{2atm}	ppm	280.1	279.9	280.2	279.9	280.1	280.0	279.9	280.0
pCO_{2l}	ppm	279.1	279.9	289.0	280.2	272.9	279.7	280.4	280.0
pCO_{2h}	ppm	283.2	280.0	253.5	280.2	320.7	281.6	276.9	279.8
O_{2d}	μmol/kg	217.1	220.6	331.6	332.3	160.9	163.3	275.4	275.4
AOU_h	μmol/kg	4.0	0.6	1.2	0.2	2.7	0.4	0.	0.
AOU_d	μmol/kg	115.8	112.3	1.2	0.2	114.4	112.1	0.	0.
$TCO_{2d} - TCO_{2l}$	μmol/kg	**332.2**	**329.7**	**141.1**	**164.7**	**116.7**	**87.2**	**81.8**	**84.1**

phosphate concentration in the polar box and the amount of phosphate that is assumed to be unutilized by the biota. This important role for PO_{4h} can be extracted directly from the model equations.

[14] Equations (1) and (2) give the TCO_2 and PO_4 balances for the deep box,

$$\frac{d}{dt}TCO_{2d} = (T + f_{hd}) \cdot (TCO_{2h} - TCO_{2d}) + r_{Corg:P} \cdot (P_l + P_h) \tag{1}$$

$$\frac{d}{dt}PO_{4d} = (T + f_{hd}) \cdot (PO_{4h} - PO_{4d}) + P_l + P_h, \tag{2}$$

where P_l and P_h are the sinking fluxes of phosphorus from the low-latitude and high-latitude surface boxes and $r_{Corg:P}$ is the C:P ratio assumed for organic matter in sinking particles. The quantities $TCO_{2h} - TCO_{2d}$ and $PO_{4h} - PO_{4d}$ on the right-hand sides of equations (1) and (2) reflect the build up of CO_2 and PO_4 concentrations in the deep box due to the remineralization of organic particles. Rearranging equation (2) to yield an expression for $P_l + P_h$, and substituting equation (2) into equation (1) at steady state, yields an equation in which these two quantities are related directly.

$$TCO_{2d} - TCO_{2h} = r_{Corg:P} \cdot (PO_{4d} - PO_{4h}). \tag{3}$$

[15] TCO_2 concentrations in the two surface boxes are linked by gas exchange with the atmospheric box. If there are no temperature differences in the system, TCO_{2l} approaches TCO_{2h} and vice versa. If gas exchange rates are also sufficiently fast, $TCO_{2l} = TCO_{2h}$. At the limit of fast gas exchange, equation (3) can be rewritten as

$$TCO_{2d} - TCO_{2l} = r_{Corg:P} \cdot (PO_{4d} - PO_{4h}). \tag{4}$$

The left-hand side of equation (4) is our metric for the strength of the organic pump. The $r_{Corg:P}$ on the right-hand side is a constant; PO_{4d} is essentially constant as well as it is fixed by the total amount of PO_4 in the system. This means that the strength of the organic pump with fast gas exchange is a function of PO_{4h} only. A low value of PO_{4h} means that there will be a large surface to deep TCO_2 difference and a strong organic pump. A high value of PO_{4h} means that there will be a small surface to deep TCO_2 difference and a weak organic pump.

[16] Equation (4) can be used to predict the fast-gas-exchange result in Table 1 and Figure 1. Substituting 2.146 μmol/kg for PO_{4d}, 1.485 for PO_{4h}, and 130 for $r_{Corg:P}$ yields a predicted surface to deep TCO_2 difference of 85.9 μmol/kg. This is very close to the actual model result, 87.2 μmol/kg. The small difference is accounted for by the fact that the 30x gas exchange rate being used in the actual model is not infinitely fast. The organic pump with normal gas exchange, 116.7 μmoles/kg, is one third stronger. The pump is stronger because finite gas exchange impedes the outgassing of remineralized CO_2 from the polar box. This is reflected in the 41-ppm sea-air pCO_2 difference and the higher TCO_2 concentration in the polar box. A higher TCO_2 concentration in the polar water filling the deep box increases the low-latitude to deep TCO_2 difference.

[17] The third panel of Figure 1 gives results for a solution in which the polar box is eliminated. This modification is carried out by setting the parameters f_{hd} and P_h to zero. With these changes, the polar box becomes an extension of the low-latitude box (with $PO_{4h} = 0$) and the three-box model is effectively a two-box model. Elimination of the polar box leads to a dramatic shift of CO_2 from the atmosphere and upper ocean boxes into the deep box. The atmospheric pCO_2 drops from 280 to 142 ppm while the strength of the organic pump more than doubles from 117 to 281 μmol/kg.

[18] In the lower two panels of Figure 1, a similar CO_2 reduction is brought about through a ten fold increase in P_h. This is the classic polar nutrient response. Enhanced biological uptake in the polar box utilizes more of the available PO_4 and drives down PO_{4h} from 1.49 to 0.37 μmol/kg. The atmospheric pCO_2 declines from 280 ppm to 164 and 156 ppm, respectively. A ten-fold increase in P_h has essentially the same effect in the full model (where

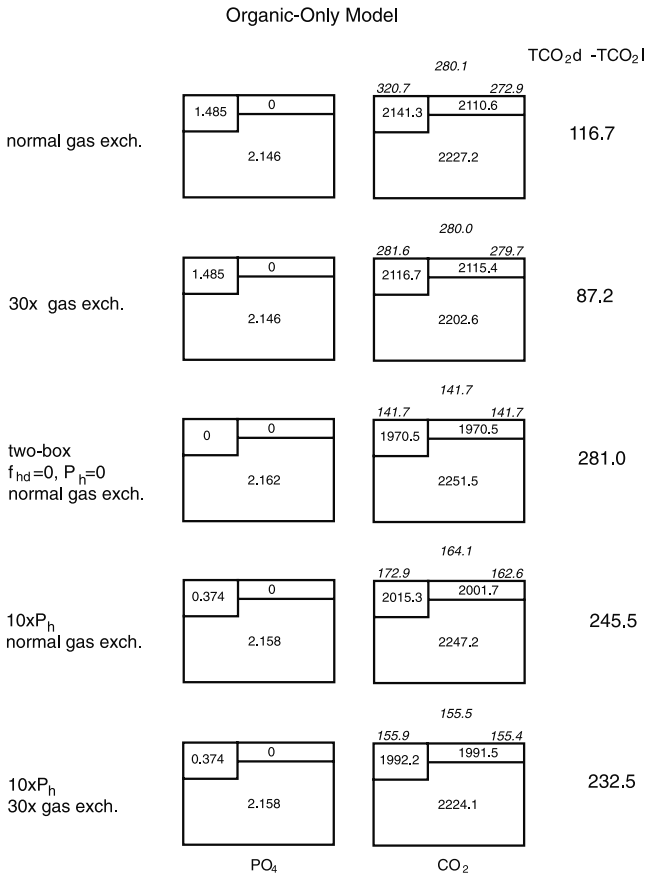

Figure 1. PO_4, TCO_2, and pCO_2 concentrations for five solutions of the organic-only version of the three-box model. The top two panels give results from the standard model with normal gas exchange and fast (30x) gas exchange. The model in the third panel has been modified so that the polar box is an extension of the low-latitude box (with PO_{4h} = 0). The polar biology factor (P_h) has been increased by 10x in the bottom two panels. The total amount of CO_2 in the two models with normal gas exchange (panels 1, 3, and 4) is kept constant at the amount given in panel 1 and in column 5 of Table 1; the total amount of CO_2 in the two models with fast gas exchange (panels 2 and 5) is kept constant at the amount given in panel 2 and in column 6 of Table 1.

solubility and carbonate effects are included) as it does in the organic-only model.

[19] Model output from Figure 1 is illustrated in a different way in Figure 2 where the properties of individual ocean boxes are plotted in a TCO_2 versus PO_4 space. Results from the standard model (1 × P_h) are plotted in the top panel. Results with the ten-fold increase in polar biological production (10 × P_h) are plotted in the bottom panel. Output from models with normal gas exchange is given in red (shaded). Output from models with fast gas exchange is given in blue (black).

[20] A set of red (dashed shaded) and blue (solid black) diagonal lines appear on each figure with the Redfield slope for organic particles ($r_{Corg:P}$ = 130:1). The chemistry of interior water parcels in an organic-only model must evolve along one of these "remineralization trajectories." One set of trajectories extends up from the polar box points. Another set extends up from the low-latitude points for reference. The deep box composition in each case lies along the polar trajectory. Two vertical bars appear on the right in each figure also coded red (dashed shaded) or blue (solid

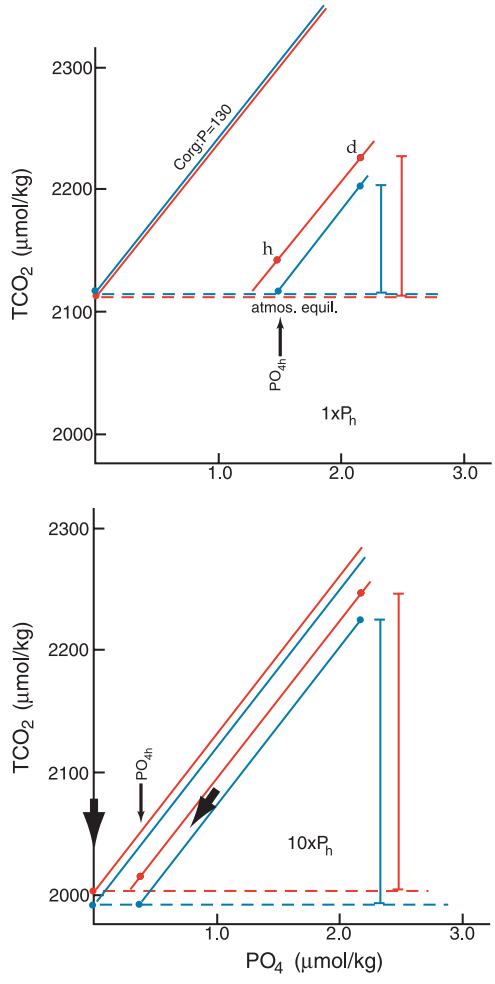

Figure 2. The organic pump in the three-box model in a TCO_2 versus PO_4 space. Box compositions (solid dots) are plotted along with remineralization trajectories with the Redfield slope, $r_{Corg:P}$ = 130. Red (shaded) dots and red (shaded dashed) trajectories are from models with normal gas exchange. Blue (black) dots and blue (solid black) trajectories are from models with fast (30x) gas exchange. The top diagram gives results from the standard model with an atmospheric pCO_2 of 280 ppm. The horizontal lines at a TCO_2 concentration of 2115 µmol/kg show the TCO_2 in equilibrium with an atmospheric pCO_2 of 280 ppm (at 10°C). The bottom diagram gives results from models in which the polar biology factor (P_h) has been increased by 10x. Color-coded vertical bars on the right give the organic pump strength for each solution, i.e., $TCO_{2d} - TCO_{2I}$. A strong pump is associated with tall vertical bars on the right and long trajectories between polar surface water and deep water.

black). The height of these bars is the TCO_2 difference between deep water and low-latitude surface water, i.e. the strength of the organic pump for each model.

[21] A low level of polar nutrient utilization, i.e., a position for PO_{4h} far to the right, means that PO_4 and TCO_2 differences between deep water and polar surface water are small. This leads to short remineralization trajectories, short vertical bars on the right, and relatively high CO_2 concentrations in the upper ocean and atmosphere. CO_2 remineralized in the interior leaks out of the deep box so that the surface ocean and deep ocean are less well differentiated in TCO_2.

[22] A high level of nutrient utilization shifts PO_{4h} to the left. This drives the polar box TCO_2, PO_4 composition down along the polar-deep remineralization trajectory. It drives the TCO_2 in the low-latitude box down as well. The vertical bars on the right become much taller. Polar surface water becomes more like low-latitude surface water and both surface water types become more differentiated from deep water. The efforts of the biota are more fully expressed: More of the CO_2 in the system resides in the deep ocean and less in the atmosphere and upper ocean.

[23] Two key features of the three-box model are illustrated in these examples; neither feature holds in the GCM to be examined next. As shown in equation (4), changes in PO_{4h} are required to change the organic pump in the three-box model. There is no other way to change the strength of the pump short of changing the amount of PO_4 in the system or changing the Redfield ratio. Finite gas exchange is also seen to have a modest effect on the strength of the organic pump; that is, the vertical bars within the two panels in Figure 2 are not all that different from each other. The gas exchange effect is relatively small for the same reason that it is was found to be small in part 1: The large area of the polar box makes the transfer of remineralized CO_2 from the polar box to the atmosphere fairly efficient. Thus the strength of the organic pump in the three-box model is set mainly by PO_{4h}, not by gas exchange factors.

3. Organic Pump in the Princeton Ocean Biogeochemistry Model (POBM)

[24] The Princeton Ocean Biogeochemistry Model (POBM) described by *Murnane et al.* [1999] is one of several GCMs examined by *Archer et al.* [2000a]. It is derived from a GCM based on the Geophysical Fluid Dynamics Laboratory Modular Ocean Model (GFDL MOM) version 1 and is described in more detail in part 1. The organic pump in the POBM is isolated in a way that is analogous to the method used in the three-box model. Surface pCO_2s and the local pCO_2 gradients between the ocean and atmosphere are calculated as if all surface temperatures are 10°C. Carbonate components of the full biology model are switched off. The effect of the virtual salt flux on PO_4, alkalinity, and TCO_2 is also switched off.

[25] The uptake of CO_2 and PO_4 into sinking particles is determined in the POBM by restoring surface PO_4 concentrations to the observed annually averaged PO_4 in every surface grid cell. In low latitudes where the observed PO_4 concentrations tend to be very low, the restoring operation removes almost all the phosphate; that is, virtually all the available PO_4 is utilized. The restoring operation in high latitudes reduces PO_4 concentrations to a much smaller degree. Some of the PO_4 goes into sinking particles and some remains unutilized in the surface water.

[26] Two versions of the organic-only POBM have been run out to compare with the box model. In the first version, the TCO_2 distribution is allowed to evolve under a fixed preindustrial atmospheric pCO_2 of 278.2 ppm using the same set of gas exchange coefficients used by *Murnane et al.* [1999]. In the second version, the TCO_2 in every surface grid cell was restored at every time step to the preindustrial equilibrium value at 10°C as a way of simulating fast gas exchange. This approach follows the approach used by Murnane et al. to produce the solubility and potential solubility models that are used in part 1.

[27] Fixing the atmospheric pCO_2 helps to simplify the analysis to follow. It does, however, lead to a nonphysical result that needs to be kept in mind. With a fixed pCO_2, a change in the strength of the organic pump makes TCO_2 concentrations in the interior rise or fall while TCO_2 concentrations at the surface remain constant. A change in the organic pump in the real world (where the total amount of CO_2 in the system must be conserved) would have the opposite effect. It would make the atmospheric pCO_2 and upper ocean TCO_2 concentrations rise and fall while TCO_2 concentrations in the deep ocean would change relatively little. They key point for this paper is that the TCO_2 difference between the surface ocean and deep ocean should rise and fall by the same amount whether the atmospheric pCO_2 is fixed or is allowed to vary.

[28] Figure 3 shows average vertical profiles of TCO_2 from the normal and fast gas exchange versions of the organic-only POBM. Surface TCO_2 concentrations are nearly identical due to the fixed atmospheric pCO_2. The surface to deep TCO_2 difference in the model with fast gas exchange is about 90 μmol/kg vs. 144 μmol/kg in the model with normal gas exchange. The 90 μmol/kg pump strength in the POBM with fast gas exchange is nearly the same as the pump strength in the box model with fast gas exchange, 87 μmoles/kg.

[29] Figure 5 in part 1 examined the air-sea CO_2 fluxes and sea-air pCO_2 differences in the solubility-only version of the POBM. It showed that much of the CO_2 flux into the ocean in high latitudes is concentrated in a few areas of the North Atlantic and Southern Ocean that have very large pCO_2 deficits in relation to the atmospheric pCO_2. The top panel of Figure 4 shows air-sea CO_2 fluxes in the organic-only version of the POBM. As in Part 1, CO_2 fluxes in polar regions tend to be concentrated in areas where the fluxes are very large (10 moles $C/m^2/yr$ or more). Sea-air pCO_2 differences are shown in the bottom panel. High-flux areas in the Southern Ocean have ΔpCO_2s in excess of 90 ppm. Sea-air pCO_2 differences in the Weddell and Ross embayments, the areas of the model where the densest bottom water is formed, are very high at about 120 ppm.

[30] The areas of the Southern Ocean with high ΔpCO_2s are areas of deep convection where subsurface water with high concentrations of remineralized CO_2 is brought up to the surface. These convective areas tend to be small. The outgassing of remineralized CO_2 is inhibited by finite gas

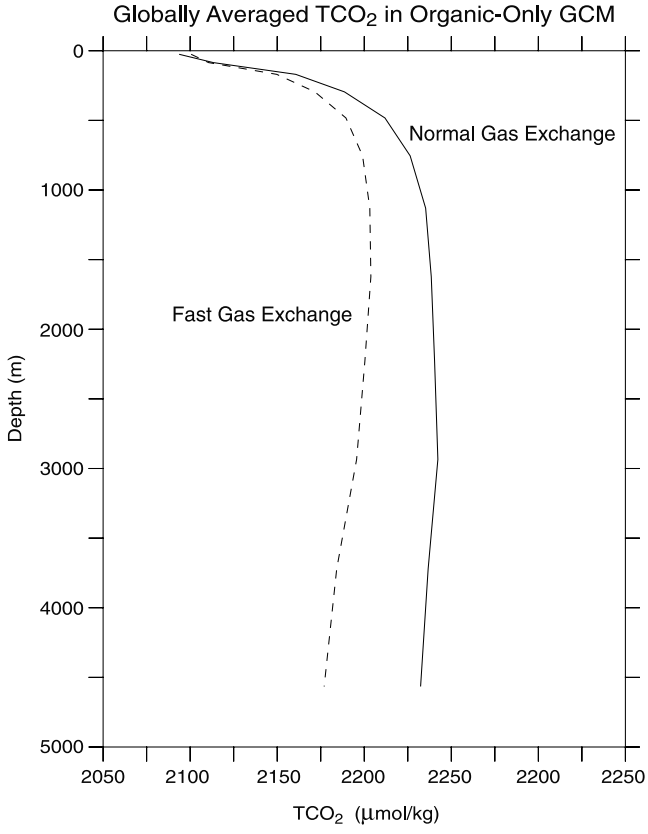

Figure 3. Vertical profiles of horizontally averaged TCO_2 in the organic-only version of the POBM (units μmol/kg). The dashed curve is from the version of the model with fast gas exchange. The solid curve is from the model with normal gas exchange. Both models were run out with the same atmospheric pCO_2 (278.2 ppm) and both have nearly the same TCO_2 concentrations at the surface. Deep water in the model with normal gas exchange has 54 μmol/kg more CO_2 than deep water with fast gas exchange.

exchange rates operating over such small areas. The limitation on outgassing drives up the surface pCO_2. Outgassing in the Weddell and Ross Seas is also inhibited by a presumed sea-ice cover. As seen in Figure 3, average deep water has a TCO_2 concentration that is elevated by 54 μmol/kg with respect to the fast gas exchange model. The deep TCO_2 excess with normal gas exchange is basically an average of the TCO_2 excess in the northern North Atlantic, which is close to zero, and the TCO_2 excess in the Weddell and Ross Seas, which is 80–90 μmol/kg.

[31] The air-sea flux pattern in the North Atlantic in Figure 4 is quite different from the air-sea flux pattern seen in Part 1. Whereas the North Atlantic north of 60°N is an important area for CO_2 uptake in the solubility-only model, it is a very unimportant area for the outgassing of remineralized CO_2. This is because the deep water formed in the North Atlantic forms north of the Icelandic sills where it is isolated from deep water in the open Atlantic. Very little remineralized CO_2 accumulates north of the sills, and very little remineralized CO_2 is brought to the surface when new deep-water forms. Thus, new NADW in the organic-only model tends to have an initial TCO_2 that stays close to equilibrium. Virtually all the outgassing of remineralized CO_2 from the deep ocean occurs in the Southern Ocean.

[32] TCO_2, PO_4 compositions for all the grid cells in the POBM are plotted in Figure 5. This is the GCM-equivalent to the top panel of Figure 2. The top panel of Figure 5 shows POBM results with normal gas exchange; the bottom panel gives results with fast gas exchange. It is easy to pick out remineralization trajectories that link surface and interior points. Trajectories that extend upward from PO_4 concentrations between 0 and 0.5 μmol/kg are composed of grid cells from the thermocline. Trajectories that extend upward from higher initial PO_4 concentrations connect high-nutrient surface waters with the deep ocean. Surface points in the bottom panel (fast gas exchange) form a clearly defined horizontal line at 2100 μmol/kg TCO_2. This is the TCO_2 concentration that is in equilibrium with the POBM's specified atmospheric pCO_2 at 10°C.

[33] The composition of new North Atlantic Deep Water (NADW) can be located in the swarm of points in the middle of the equilibrium line with a PO_4 concentration of 0.9 μmol/kg. The POBM's initial PO_4 for NADW is very close to the observed NADW composition. Antarctic Bottom Water (AABW) is identified by the swarm of points at the high-PO_4 end of the equilibrium line. The POBM's initial PO_4 for AABW, 2.0 μmol/kg, is a bit low; the actual value is about 2.15 μmol/kg. The most distinct difference between the two panels of Figure 5 can be traced to the vertical position of AABW. The cloud of AABW points in the model with normal gas exchange lies well above the atmospheric equilibrium line. Thus, southern deep water with the highest initial PO_4 concentrations comes into contact with the atmosphere with a TCO_2 concentration of about 2185 μmol/kg. The TCO_2 of new NADW plots just above the equilibrium line at about 2110 μmol/kg.

4. A New Theoretical Framework for the Organic Pump

[34] The polar box in the three-box model is supposed to behave like an average polar region in the real ocean. In this regard, PO_{4h} in the three-box model, 1.5 μmol/kg, lies halfway between the initial PO_4 concentrations of NADW and AABW in the POBM, 0.9 and 2.0 μmol/kg, respectively. This bit of convergence explains why the surface to deep TCO_2 difference in the three-box model with fast gas exchange, 87 μmoles/kg, is nearly identical to surface to deep TCO_2 difference in the POBM with fast gas exchange, 90 μmoles/kg.

[35] This bit of convergence also tends to hide a very important distinction between the three-box model, on the one hand, and the real ocean and POBM on the other. PO_{4h} in the three-box model, at 1.5 μmol/kg, is significantly depleted with respect to the PO_4 concentration in the deep box, at 2.15 μmol/kg. This level of depletion is presumed to be the result of local processes in the polar box, i.e., biological uptake that lowers the PO_4 content of the water in the polar box, or polar stratification that limits mixing with deep water and allows the biological uptake to deplete the surface PO_4. Local processes do not appear to have this kind of influence in setting the properties of new deep water

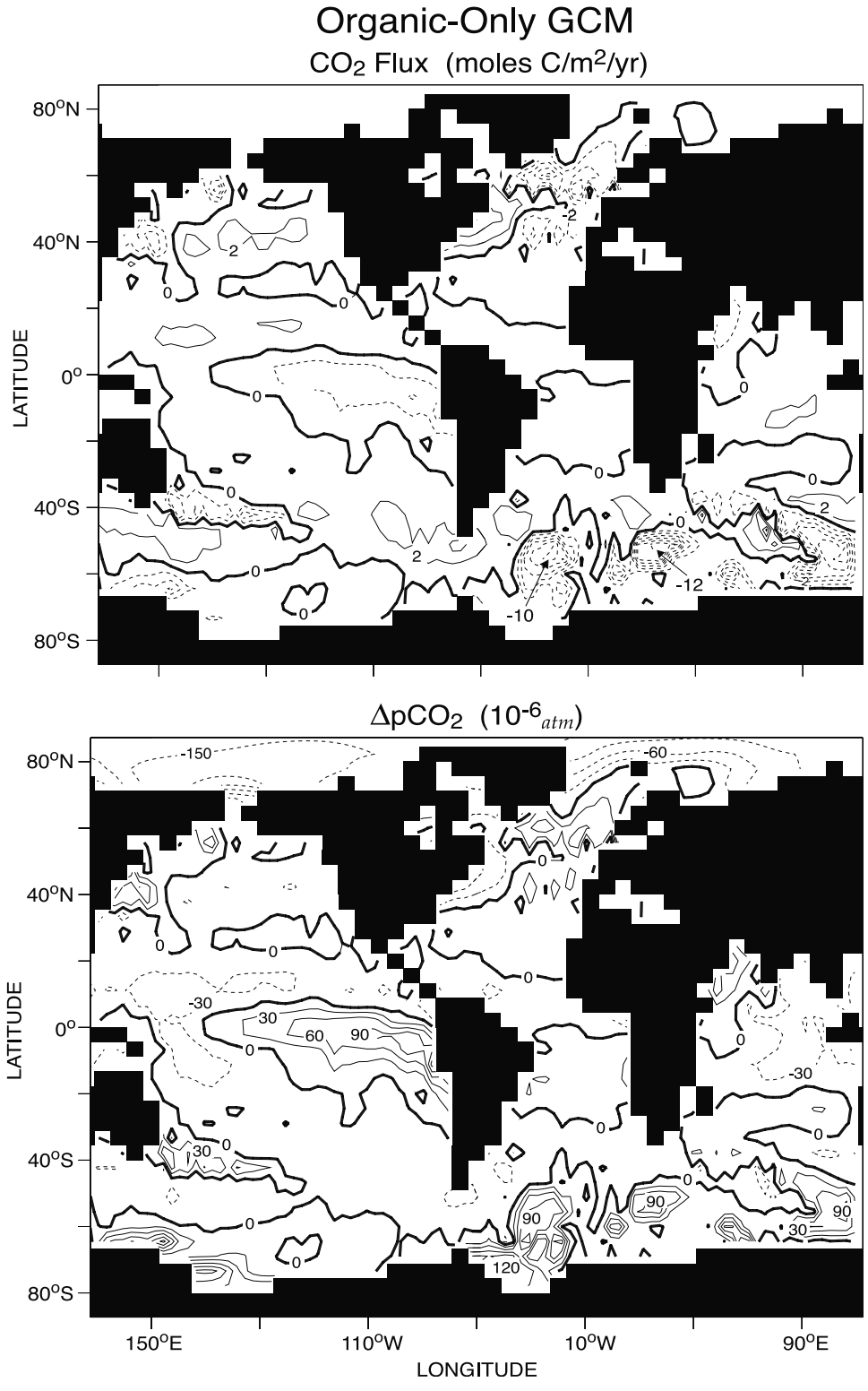

Figure 4. (top) Air-sea CO_2 fluxes in the organic-only POBM with normal gas exchange. CO_2 is coming out of the ocean in areas with negative (dashed) contours. Contour interval is 2 moles/m^2/yr. (bottom) Sea-air pCO_2 differences (contour interval = 30×10^{-6} atm). Oceanic pCO_2s are less than the atmospheric pCO_2 in areas with negative (dashed) contours. Outgoing CO_2 fluxes in the Southern Ocean are concentrated in areas of deep convection with ΔpCO_2s in excess of 90×10^{-6} atm.

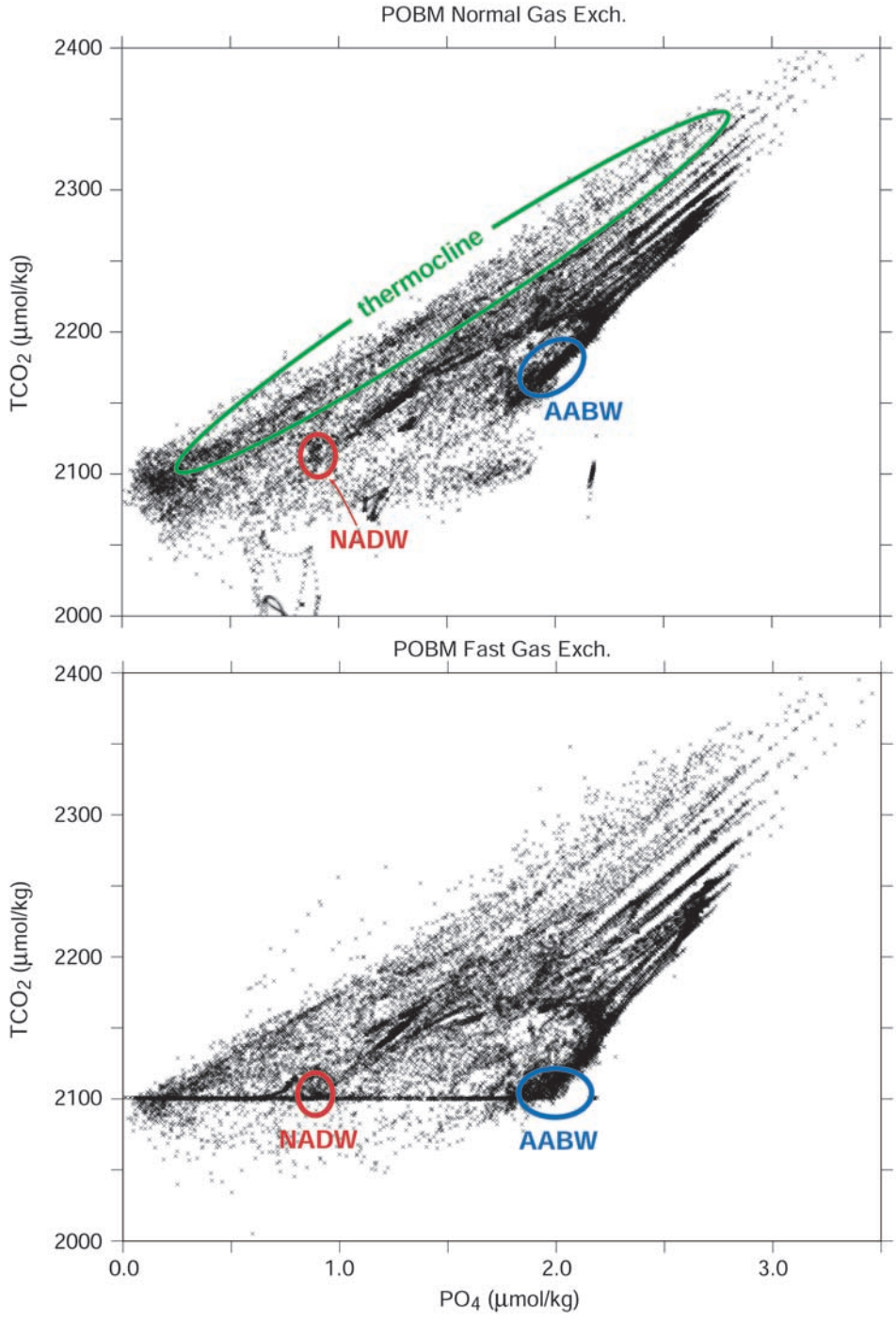

Figure 5. TCO_2 versus PO_4 scatterplot for all grid cells in the organic-only version of the POBM. The Redfield slope, $r_{Corg:P}$, is readily apparent in the trajectories for interior points. Colored (shaded) circles highlight the initial compositions of NADW and AABW. The top panel gives results from the model with normal gas exchange. The bottom panel gives results from the model with fast gas exchange. Surface points from the model with fast gas exchange form a clearly delineated horizontal line.

in the real ocean. The initial PO_4 of new AABW, at 2.15 μmol/kg, is hardly depleted at all with respect to PO_4 concentrations in deep water below the Antarctic pycnocline, 2.3 μmol/kg. The initial PO_4 of new NADW, at 0.9 μmol/kg, is strongly depleted with respect to average deep water. No one, however, would ever describe the PO4 depletion in NADW as the result of a local process: The upper ocean water masses that are converted into NADW in the real ocean are depleted in PO_4 long before they reach the northern North Atlantic.

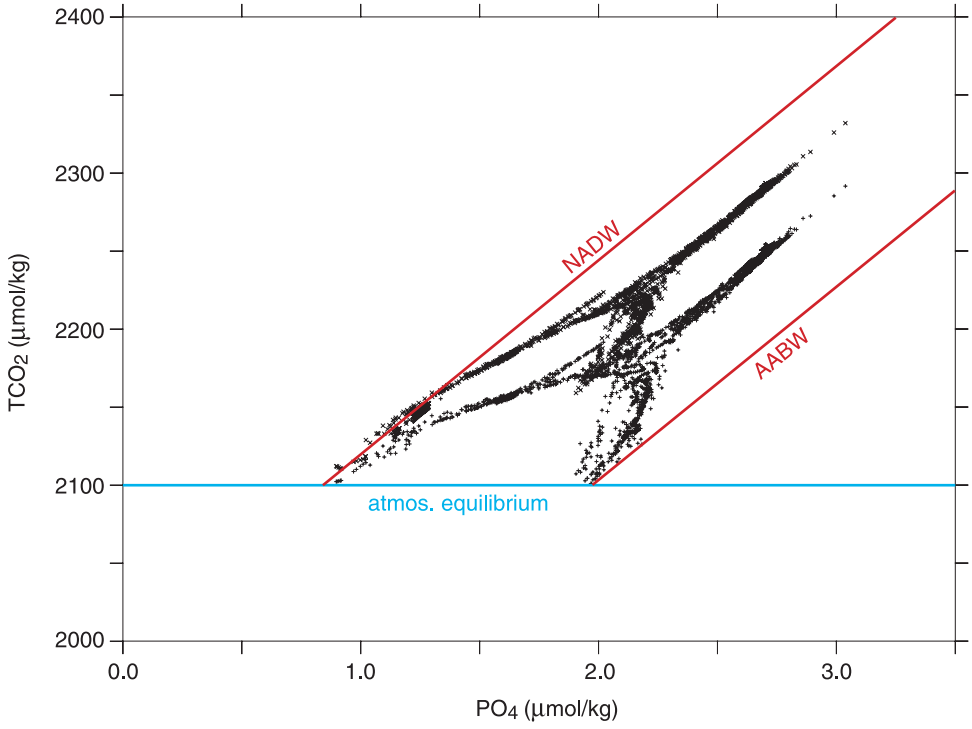

Figure 6. TCO_2, PO_4 composition of all POBM grid cells at level 9 (2228 m) showing the influence of NADW and AABW on the composition of bulk deep water. Results with normal and fast gas exchange are included in the same plot. Bulk deep water from the model with normal gas exchange has about 50 µmol/kg more TCO_2. The blue (shaded) horizontal line gives the surface equilibrium TCO_2 for both models. The red (shaded) diagonal lines show the chemical evolution of unblended NADW and AABW. As such, they define the upper and lower limits for the strength of the organic pump. The model output in the figure is biased toward the strong pump limit because all the points shown here come from one depth level only (level 9). Points from levels 10–12 are more influenced by AABW. Had they been added to the figure, the points from levels 10–12 would shift the bulk composition toward the weak pump limit.

[36] The three-box model was seen as a great breakthrough in its day because it showed that the ocean's biogeochemical system has the capacity to reduce atmospheric CO_2 without major changes in ocean chemistry or biological production. The mechanism for exercising this capacity is increased polar nutrient utilization. The organic-only POBM shows that the carbon system in the real ocean has the capacity to reduce atmospheric CO_2 without changes in polar nutrient utilization. Basically, the organic pump in the real ocean has strong and weak limits that exist because the ocean forms deep water in the north and south with different initial PO_4 concentrations.

[37] Figure 6 shows a subset of the TCO_2 vs. PO_4 results from the POBM in Figure 5 from a depth where the combined influences of NADW and AABW are most evident (2228 m, level 9). Points from both the normal and fast gas exchange models are shown together in the same plot. The swarm of TCO_2, PO_4 points from each model takes the shape of a pitchfork or trident that has a pair of outer prongs but none in the center. The outer prongs of the pitchforks map out the TCO_2, PO_4 evolution in areas close to the formation areas of NADW and AABW. The handles of the pitchforks represent the evolution of bulk deep water that is a blend of water from the two sources.

[38] Two diagonal lines have been added to Figure 6. These extend up from the equilibrium line at the initial PO_4 concentrations for NADW and AABW. The diagonal lines are remineralization trajectories for unblended NADW and AABW, respectively. If all the deep water in the POBM started out as fully equilibrated NADW, the TCO_2, PO_4 evolution of all the deep points in the model would lie along the upper diagonal line. Similarly, if all the deep water started out as fully equilibrated AABW, all the deep points would lie along the lower diagonal line. The composition of bulk deep water is constrained to lie between the two diagonal lines. The prongs from the fast gas exchange model parallel the unblended NADW and AABW trajectories before the water in the prongs mixes together to become bulk deep water.

[39] The diagonal lines in Figure 6 are the natural limits for the organic pump in the POBM. A position for bulk deep water close to the NADW trajectory indicates that the organic pump lies close to the strong pump limit, i.e., bulk deep water has a high TCO_2 in relation to equilibrated surface water. A position for bulk deep water close to the AABW trajectory indicates that the organic pump lies close to the weak pump limit; that is, bulk deep water has a low TCO_2 in relation to equilibrated surface water.

[40] The range of possible pump strengths in the ocean can be expressed algebraically as

$$\Delta TCO_{2d} = r_{Corg:P} \cdot (initialPO_{4AABW} - initialPO_{4NADW}), \quad (5)$$

where ΔTCO_{2d} is the vertical difference between TCO_2 concentrations along the two trajectories. ΔTCO_{2d} in equation (5) defines the range of possible surface to deep TCO_2 differences. With $r_{Corg:P} = 130$ and initial PO_4 levels for AABW and NADW of 2.0 and 0.9 μmol/kg, the range in possible pump strengths is 140 μmol/kg. The spread in initial PO_4 clearly sets the range. A smaller spread in initial PO_4 would reduce the range of possible pump strengths.

[41] The two states of the POBM in Figure 6 are differentiated by a thirty-fold difference in gas exchange rates. Points from the fast gas exchange model plot closer to the weak pump limit while the points from the normal gas exchange model plot closer to the strong pump limit. A more practical way to imagine different states of the organic pump in the real ocean is through changes in circulation that favor the production of NADW or AABW. An ocean that produces a dense, well-equilibrated southern bottom water that fills much of the deep ocean will have an organic pump close to the weak pump limit. An ocean that produces mainly NADW will have an organic pump close to the strong pump limit.

5. Discussion

5.1. Initial PO_4 and the Ocean's Overturning Circulations

[42] Initial PO_4 is a property of precursor water masses that are modified to become new deep water. It is not unlike salinity in this regard. Salinity in this context would be diagnostic of the evaporation and precipitation that affects precursor water masses during their transit toward the poles. Initial PO_4 is diagnostic of a precursor water mass's exposure to biological activity. The biological exposure that determines a water mass's initial PO_4 depends to a large extent on where the upwelling and sinking occur within a given overturning system.

[43] It now appears that most of the water upwelling from the deep ocean consists of Circumpolar Deep Water that reaches the surface as part of the wind-driven upwelling in the Antarctic Circumpolar Current [*Toggweiler and Samuels*, 1993; *Doos and Coward*, 1997; *Sloyan and Rintoul*, 2001; *Webb and Suginohara*, 2001]. Upwelled CDW has one of two fates. Some advects southward and is converted into deep and bottom water around the perimeter of Antarctica. Some is carried northward as part of the surface Ekman layer in the ACC. The latter component is pumped down into the main thermocline north of the ACC and is eventually converted back into deep water in the North Atlantic [*Gnanadesikan*, 1999]. The upwelling of CDW in the ACC closes the overturning circulations initiated by sinking in both the Northern and Southern Hemispheres.

[44] Because of the close proximity of the upwelling and sinking branches of the southern overturning circulation, "southern" CDW reenters the deep ocean with only a few percent of its PO_4 removed by organisms. This precursor has almost no exposure to biological activity and the deep water formed from southern CDW ends up with a high initial PO_4. With little exposure to biological activity the southern overturning circulation produces few organic particles. The northern overturning circulation, also known as the conveyor circulation of *Broecker* [1991], is different because of the vast distance between its upwelling and sinking branches. "Northern" CDW is exposed to a great deal of biological activity during its long transit back to the north. The stripping of PO_4 from northern CDW generates lots of organic particles and leaves new NADW with a low initial PO_4.

[45] As seen in the POBM, water from the northern and southern circulations is mixed together in the deep ocean so that the two water types are essentially undifferentiable when upwelling back to the surface as CDW. This merging of the two water types in the deep ocean is very important for the organic pump. It means that the pumping action associated with the productive northern overturning circuit can be undone by the lack of pumping in the unproductive southern circuit. It means that the CO_2 remineralized from the organic particles generated by the productive northern circuit can leak out to the atmosphere via the unproductive southern circuit. In this way, less remineralized CO_2 is retained in the deep water of today's ocean.

5.2. A Recipe for the Glacial Ocean

[46] The simplest way to make the deep ocean retain more CO_2 is to knock out the southern overturning system that allows so much remineralized CO_2 to escape from the deep ocean. With no southern deep water being added to the deep ocean, all the deep water in the ocean is forced to lie along the low-initial PO_4 NADW trajectory, effectively shifting the organic pump to the strong pump limit. Three recent papers have suggested a scenario similar to this one to explain the low CO_2 levels of the glacial atmosphere, but none of the authors of these papers realized that the CO_2 reduction in their respective models was related in a very simple way to the formation and circulation of northern and southern deep water.

[47] *Toggweiler* [1999] and *Gildor et al.* [2002] constructed box models of the carbon system that featured an overturning circulation inspired by the ACC effect. They showed that a sharp reduction in the vertical exchange of surface and deep waters in the Southern Ocean in conjunction with the upwelling of northern deep water next to Antarctica could account for the full amplitude of glacial-interglacial CO_2 changes. They also showed that atmospheric CO_2 could be dramatically reduced without changes in polar nutrient utilization or changes in Southern Ocean nutrient concentrations.

[48] The box model of *Stephens and Keeling* [2000] took advantage of the same ACC-inspired circulation. Stephens and Keeling showed that remineralized CO_2 could be trapped in the deep ocean by a massive reduction in gas exchange in the Southern Ocean. They argued that a complete sea-ice cover in the glacial Southern Ocean could bring about the observed CO_2 drawdown. The Stephens and Keeling mechanism basically knocks out the influence of the southern overturning by dramatically increasing the air-sea disequilibrium in the deep water being formed in the south.

[49] These papers were basically written within the context of the box-model literature in which polar nutrient concentrations are assumed to be major variables in the carbon system. The fact that atmospheric CO_2 might change in these models without changes in polar nutrient concentrations was seen as a major surprise. We would argue here that polar nutrient concentrations, specifically the initial PO_4 concentrations in new deep water, are properties that are derived from the geometry of the large-scale circulation. They are not as susceptible to modification by polar processes as they are in box models. It is more likely that the main variable in the organic pump is the mix of northern and southern deep water that determines how much of the deep ocean is ventilated through the unproductive southern loop.

[50] One of the most popular ideas associated with the glacial-interglacial CO_2 changes is the iron hypothesis of *Martin* [1990]. Martin proposed that iron in atmospheric dust lowers atmospheric CO_2 during glacial periods by enhancing the biological production in the Southern Ocean. It is very unlikely that Martin was right. Martin imagined that the organic pump works the way it does in the three-box model. He assumed, like everyone else at the time, that organic production in polar surface waters all around Antarctica should have an impact on the global pump. However, the only Antarctic production that can strengthen the global pump in a significant way is production that might reduce the initial PO_4 in new AABW in relation to NADW. Given the proximity of CDW upwelling to the deep-water formation areas on the Antarctic shelves, it is hard to see how organic production, with iron or without iron, can significantly alter the initial PO_4. Organic production in areas remote from the areas of AABW formation should not have very much effect on the organic pump.

5.3. How Well Equilibrated is New AABW in the Modern Ocean?

[51] Atmospheric CO_2 concentrations have varied between 200 and 280 ppm during full glacial and interglacial phases of the last four glacial cycles [*Petit et al.*, 1999]. The 80-ppm range is more or less the same in each of the cycles. Colder ocean temperatures account for some of the 80-ppm decrease during each of the glacial cold periods [*Heinze et al.*, 1991; *Bacastow*, 1996], but most of the CO_2 decrease occurs in response to a strengthened organic pump. The nonthermal part of the atmospheric CO_2 decrease requires an increase in the surface to deep gradient in TCO_2 of about 80 μmol/kg [e.g., *Toggweiler*, 1999].

[52] An 80-μmol/kg increase in the surface to deep TCO_2 gradient falls easily within the 140-μmol/kg range of possible pump strengths given by equation (5). However, the potential to make the organic pump 80-μmol/kg stronger depends on the state of the modern organic pump in relation to the weak-pump limit. Proximity to the weak pump limit is enhanced by an AABW composition that is well equilibrated with respect to atmospheric CO_2. Is new AABW really this well equilibrated?

[53] This is a key area where box models and GCMs tend to differ. As pointed out in Part 1 area and sea-ice restrictions lead to large solubility-induced pCO_2 deficits in the POBM. The same restrictions lead to a large organic pCO_2 excess. As seen in Figure 5, the 120-ppm pCO_2 excess in the model's Weddell Sea elevates the TCO_2 of new AABW by about 85 μmol/kg with respect to atmospheric equilibrium, which shifts the composition of the deep ocean close to the strong pump limit. If the real ocean operated this way the amplitude of glacial-interglacial CO_2 variations would probably lie outside the range that could be explained by changes in deep-water formation.

[54] Weddell Sea Bottom Water (WSBW) is the densest water mass produced around Antarctica today and is the main component of AABW. It forms on the continental shelves in the southern and western parts of the Weddell Sea [*Foldvik et al.*, 1985; *Gordon et al.*, 1993; *Orsi et al.*, 1999] from upwelled Circumpolar Deep Water (CDW) that is loaded with remineralized CO_2. How much of the remineralized CO_2 in CDW is lost to the atmosphere before new WSBW sinks from the Weddell shelf?

[55] *Weiss et al.* [1992], and T. Takahashi (personal communication, 2001) have measured the pCO_2 in surface waters in the eastern Weddell Sea during Austral winter. CO_2 fluxes during the winter (when biological production is inactive) are uniformly out of the ocean in the Weddell Sea. Wintertime pCO_2s on the eastern Weddell shelf, according to Weiss et al., exceed the atmospheric pCO_2, but not by much, 20–45 ppm.

[56] The small excess pCO_2 measured in Weddell Sea surface water is the sum of solubility, organic, and carbonate effects. We assume, following Table 1, that the carbonate pump has a small effect on the measured pCO_2 excess in the Southern Ocean. This means that the measured pCO_2 excess on the eastern Weddell shelf is the combination of a solubility-induced pCO_2 deficit and an organic pCO_2 surplus. In Part 1 we showed that a preformed solubility-induced deficit of some 60–70 ppm is brought into the Southern Ocean via the NADW component in CDW. Because there is relatively little cooling during the last stages of AABW formation, we assumed that there should be an overall reduction in the preformed deficit on the Antarctic shelves; that is, gas exchange should be able to erase the solubility deficit more than local cooling can enhance it.

[57] We estimated that the solubility-induced deficit in new bottom water might be about 30–40 ppm. If so, then the excess pCO_2 on the Weddell shelf due to organic cycling would be 50 to 85 ppm, i.e., the difference between the 20–45 ppm measured pCO_2 excess and the 30–40 ppm solubility deficit. An organic pCO_2 excess of 50–85 ppm is larger than the 41-ppm excess in the three-box model (Figure 1) but is small in relation to the 120-ppm excess in the Weddell Sea in the POBM (Figure 4).

[58] T. Takahashi (personal communication, 2001) reports that CDW near Antarctica has a pCO_2 of about 500 ppm when normalized to have the same temperature as Antarctic surface waters. The atmosphere at the time of Takahashi's measurements had a pCO_2 of 350 ppm. We estimated in Part 1 that average deep water has an pCO_2 deficit due to solubility effects of 50–60 ppm, halfway between the pCO_2 deficit in NADW and our estimated deficit for AABW. The excess pCO_2 in CDW due to organically cycled CO_2 is then $500 - 350 + (50 - 60) = 200 - 210$ ppm. This figure can

be compared to the 50–85 ppm estimate above for the organic pCO_2 excess in Weddell shelf water. A reduction of the organic pCO_2 excess from 200–210 ppm to 50–80 ppm suggests that 60 to 75% of the remineralized CO_2 in CDW has been discharged to the atmosphere before new WSBW sinks from the Weddell shelf.

[59] Isopycnals associated with CDW rise south of the Antarctic Circumpolar Current such that CDW is found at relatively shallow depths (200–600 m) next to Antarctica. Contact between the atmosphere and CDW is blocked by the overlying Antarctic pycnocline but CDW is known to mix with remnant winter mixed-layer water as it is absorbed upward into the pycnocline [*Martinson and Ianuzzi*, 1998]. A blend of CDW and winter surface water finally flows onto the Antarctic shelves. Most of the heat loss associated with the cooling of CDW seems to occur before this modified CDW ever reaches the Antarctic shelves. The same should be true for the venting of remineralized CO_2.

[60] The idea that the organic pCO_2 excess in new WSBW is moderately small is supported by $\delta^{13}C$ measurements. WSBW has a $\delta^{13}C$ content of 0.8‰, a value that is substantially higher than the $\delta^{13}C$ content of CDW, 0.3–0.4‰ [*Mackensen et al.*, 1993, 1996]. The relatively high $\delta^{13}C$ of WSBW is a good indication that air-sea gas exchange has reset the $\delta^{13}C$ of WSBW toward the $\delta^{13}C$ of atmospheric CO_2. The air-sea equilibration time for $\delta^{13}C$ is much slower than for CO_2 [*Broecker and Peng*, 1974]. The fact that one sees any evidence at all for $\delta^{13}C$ equilibration is a good indication that the CO_2 content of WSBW has been reset a fairly long way toward atmospheric equilibrium.

[61] In summary, the solubility-induced pCO_2 deficit in new southern deep water is unknown and is a critical factor in this analysis. If the solubility deficit in new AABW is fairly small, as estimated here, the excess pCO_2 due to organic cycling (calculated by difference from the observed excess pCO_2) should also be moderately small. A moderately small excess pCO_2 means that the strength of the organic pump of the modern ocean is not far from the weak pump limit. If so, the low levels of atmospheric CO_2 during glacial time could be explained by nothing more than a change in deep-water formation that eliminates the influence of high-PO_4 southern deep water.

5.4. Polar Nutrient Response

[62] The debate that initiated this work began with the observation that reductions in polar nutrient concentrations have more impact on atmospheric CO_2 in box models than in GCMs [*Heinze et al.*, 1991; *Archer et al.*, 2000a]. The Polar Skeptics suggested that this difference in model behavior arises because there are unresolved mixing and circulation features in the real ocean and in GCMs that are missing in box models. The Skeptics documented large differences in the solubility behavior of box models and GCMs and claimed that the missing features could account for the solubility differences. They then inferred that the missing features would account for differences in polar nutrient response.

[63] We have shown that the main solubility difference between box models and GCMs is caused by differences in air-sea CO_2 equilibration. These differences are due primarily to differences in the effectiveness of gas exchange in polar outcrops where new deep water is formed. They are not due to missing circulation and mixing features. Poor air-sea CO_2 equilibration in the Southern Ocean leaves the solubility pump in the POBM too weak in relation to the real ocean and leaves the organic pump too strong.

[64] We suspect, but have not demonstrated, that differences in air-sea equilibration can explain the differences in polar nutrient response in box models and GCMs. A good test of this idea would be a series of polar nutrient reduction experiments in an organic-only setting. These experiments could be used to evaluate the shift in the bulk composition of the deep ocean in relation to the strong- and weak-pump limits. A reduction in Southern Ocean nutrient concentrations may not have a large effect on atmospheric CO_2 if the organic pump is too strong; that is, if the initial PO_4, TCO_2 composition of AABW plots well off the atmospheric equilibrium line and close to the remineralization trajectory for NADW (as seen for the POBM in Figures 5 and 6). The key point, however, is that the need to reduce polar nutrients is not as great as it was once thought to be. The strength of the organic pump appears to be set by the large-scale circulation. Changes in circulation would seem to be a more feasible way to alter the pump than reductions in polar nutrients.

6. Conclusions

[65] One of the reasons why the glacial-interglacial cycles in atmospheric CO_2 have proven to be so hard to understand is that our tools for describing the ocean's carbon system have sent us off in different directions. The three-box model tells us to search for evidence of enhanced nutrient utilization in polar areas. GCMs seem to be telling us to search for evidence for enhanced organic production for the ocean as a whole. According to the Polar Skeptics [*Bacastow*, 1996; *Broecker et al.*, 1999; *Archer et al.*, 2000a], this muddled message keeps coming out because box models and GCMs represent the carbon cycle in fundamentally different ways. The problem, they claim, lies with box models that are too polar-dominated. This characterization is not borne out in our analysis of the three-box model and the Princeton Ocean Biogeochemistry Model (POBM).

[66] The main difference between box models and GCMs seems to be the degree of air-sea CO_2 equilibration in new deep water. This is not a fundamental difference. New deep water in box models is probably too well equilibrated because the area given over to their polar boxes is too large. This makes the solubility pump too strong and the organic pump too weak in relation to the real ocean. Southern deep water in GCMs, on the other hand, tends to be poorly equilibrated. This is because the area available for gas exchange is very small and because gas exchange in these areas may be limited in an unrealistic way by a presumed sea-ice cover. This tendency makes the solubility pump too weak and the organic pump too strong. Although it is impossible to say with certainty what the initial ΔpCO_2s of AABW actually is with respect to the separated pumps, the attributes identified here suggest that the three-box

model and the POBM have bracketed the level of disequilibrium in the real ocean.

[67] If there is a fundamental box model-GCM difference, it is the difference between the three- box model, with its one polar box, and all other models that have distinct northern and southern polar regions. Polar nutrient depletion is the only avenue for producing a stronger organic pump in the three-box model. The organic pumps in GCMs and in the real ocean have natural upper and lower limits that are set by the initial PO_4 concentrations in the deep water formed in the North Atlantic and in Southern Ocean. The strength of the organic pump can swing between these limits via changes in deep-water formation that alter the mix of northern and southern deep water filling the deep ocean. The north-south spread in initial PO_4 would seem to be wide enough to account for the full amplitude of glacial-interglacial changes in atmospheric CO_2.

[68] The Skeptics are right to question polar nutrient depletion as a mechanism for lowering atmospheric CO_2. They are off target in their general depreciation of the ocean's polar regions. The fact that the ocean produces two types of deep water with very different levels of initial PO_4 would seem to be the mother lode of organic pump variability.

[69] **Acknowledgments.** The authors thank Roberta Hotinski and Ben McNeil for their internal reviews of the manuscript. We would also like to acknowledge an important contribution made by David Archer. In a note written to J. R. T. in June 2000, David insisted that the organic pump mechanism at work in the seven-box model of *Toggweiler* [1999] is based on a shift of equilibrated deep-water formation from the Southern Ocean, where the initial PO_4 is high, to the North Atlantic, where the initial PO_4 is low. This was a prescient observation that describes in a very simple way how the organic pump can be strengthened in both the *Toggweiler* [1999] box model and the POBM. A. G. and J. L. S. would like to acknowledge support for the Carbon Modeling Consortium from NOAA's Office of Global Programs (grant NA96GP0312).

References

Archer, D. E., and E. Maier-Reimer, Effect of deep sea sedimentary calcite preservation on atmospheric CO_2, *Nature*, *367*, 260–264, 1994.

Archer, D. E., G. Eshel, A. Winguth, W. Broecker, R. Pierrehumbert, M. Tobis, and R. Jacob, Atmospheric pCO_2 sensitivity to the biological pump in the ocean, *Global Biogeochem. Cycles*, *14*, 1219–1230, 2000a.

Archer, D., A. Winguth, D. Lea, and N. Mahowald, What caused the glacial/interglacial atmospheric pCO_2 cycles?, *Rev. Geophys.*, *38*, 159–189, 2000b.

Bacastow, R. B., The effect of temperature change of the warm surface waters of the oceans on atmospheric CO_2, *Global Biogeochem. Cycles*, *10*, 319–333, 1996.

Broecker, W. S., Glacial to interglacial changes in ocean chemistry, *Prog. Oceanogr.*, *11*, 151–197, 1982.

Broecker, W. S., The great ocean conveyor, *Oceanography*, *4*, 79–89, 1991.

Broecker, W. S., and G. M. Henderson, The sequence of events surrounding Termination II and their implications for the cause of glacial-interglacial CO_2 changes, *Paleoceanography*, *13*, 352–364, 1998.

Broecker, W. S., and T.-H. Peng, Gas exchange rates between air and sea, *Tellus*, *26*, 21–35, 1974.

Broecker, W., J. Lynch-Stieglitz, D. Archer, M. Hoffmann, E. Maier-Reimer, O. Marchal, T. Stocker, and N. Gruber, How strong is the Harvardton-Bear constraint?, *Global Biogeochem. Cycles*, *13*, 817–821, 1999.

Doos, K., and A. Coward, The Southern Ocean as the major upwelling zone for North Atlantic Deep Water, *Int. WOCE Newsl. July*, 3–4, 1997.

Foldvik, A., T. Gammelsrod, and T. Torrensen, Circulation and water masses on the southern Weddell Sea Shelf, in *Oceanology of the Antarctic Continental Shelf*, *Antarct. Res. Ser.*, vol. 43, edited by S. S. Jacobs, pp. 5–20, AGU, Washington, D. C., 1985.

Gildor, H., E. Tziperman, and J. R. Toggweiler, Sea ice switch mechanism and glacial- interglacial CO_2 variations, *Global Biogeochem. Cycles*, *16*, 1032, doi:10.1029/2001GB001446, 2002.

Gnanadesikan, A., A simple predictive model for the structure of the oceanic pycnocline, *Science*, *283*, 2077–2079, 1999.

Gordon, A. L., B. A. Huber, H. H. Hellmer, and A. Ffield, Deep and bottom water of the Weddell Sea's western rim, *Science*, *262*, 95–97, 1993.

Heinze, C., E. Maier-Reimer, and K. Winn, Glacial pCO_2 reduction by the World Ocean: Experiments with the Hamburg Carbon Cycle Model, *Paleoceanography*, *6*, 395–430, 1991.

Knox, F., and M. B. McElroy, Changes in atmospheric CO_2: Influence of the marine biota at high latitude, *J. Geophys. Res.*, *89*, 4629–4637, 1984.

Mackensen, A., H.-W. Hubberten, T. Bickert, G. Fischer, and D. K. Futterer, The $\delta^{13}C$ in benthic foraminiferal tests of Fontbotia Wuellerstorfi relative to the $\delta^{13}C$ of dissolved inorganic carbon in Southern Ocean deep water: Implications for glacial ocean circulation models, *Paleoceanography*, *8*, 587–610, 1993.

Mackensen, A., H.-W. Hubberten, N. Scheele, and R. Schlitzer, Decoupling of $\delta^{13}C$ and phosphate in recent Weddell Sea deep and bottom water: Implications for glacial Southern Ocean paleoceanography, *Paleoceanography*, *11*, 203–215, 1996.

Martin, J. H., Glacial-interglacial CO_2 change: The iron hypothesis, *Paleoceanography*, *5*, 1–13, 1990.

Martinson, D. G., and R. A. Ianuzzi, Antarctic ocean-ice interactions: Implications from ocean bulk property distributions in the Weddell gyre, in *Antarctic Sea Ice: Physical Processes, Interactions, and Variability*, *Antarct. Res. Ser.*, vol. 74, edited by M. O. Jeffries, pp. 243–271, AGU, Washington, D. C., 1998.

Murnane, R. J., J. L. Sarmiento, and C. LeQuere, Spatial distribution of air-sea CO_2 fluxes and the interhemispheric transport of carbon by the oceans, *Global Biogeochem. Cycles*, *13*, 287–305, 1999.

Orsi, A. H., G. C. Johnson, and J. L. Bullister, Circulation, mixing, and production of Antarctic Bottom Water, *Prog. Oceanogr.*, *43*, 55–109, 1999.

Petit, J. R., et al., Climate and atmospheric history of the past 420,000 years from the Vostok ice core, Antarctica, *Nature*, *399*, 429–436, 1999.

Sarmiento, J. L., and J. C. Orr, Three-dimensional simulations of the impact of Southern Ocean nutrient depletion on atmospheric CO_2 and ocean chemistry, *Limnol. Oceanogr.*, *36*, 1928–1950, 1991.

Sarmiento, J. L., and J. R. Toggweiler, A new model for the role of the oceans in determining atmospheric CO_2, *Nature*, *308*, 621–624, 1984.

Siegenthaler, U., and T. Wenk, Rapid atmospheric CO_2 variations and ocean circulation, *Nature*, *308*, 624–626, 1984.

Sloyan, B. M., and S. R. Rintoul, The Southern Ocean limb of the global deep overturning circulation, *J. Phys. Oceanogr.*, *31*, 143–173, 2001.

Stephens, B. B., and R. F. Keeling, The influence of Antarctic sea ice on glacial-interglacial CO_2 variations, *Nature*, *404*, 171–174, 2000.

Toggweiler, J. R., Variation of atmospheric CO_2 by ventilation of the ocean's deepest water, *Paleoceanography*, *14*, 571–588, 1999.

Toggweiler, J. R., and B. Samuels, New radiocarbon constraints on the upwelling of abyssal water to the ocean's surface, in *The Global Carbon Cycle*, *NATO ASI Ser.*, edited by M. Heimann, pp. 333–366, Springer-Verlag, New York, 1993.

Toggweiler, J. R., A. Gnanadesikan, S. Carson, R. Murnane, and J. L. Sarmiento, Representation of the carbon cycle in box models and GCMs, 1, Solubility pump, *Global Biogeochem. Cycles*, *17*, doi:10.1029/2001GB001401, 2003.

Webb, D. J., The interior circulation of the ocean, in *Ocean Circulation and Climate*, edited by G. Siedler, J. Church, and J. Gould, pp. 205–213, Academic, San Diego, Calif., 2001.

Weiss, R. F., F. A. Van Woy, and P. K. Salemeh, Surface water and atmospheric carbon dioxide and nitrous oxide observations by shipboard automated gas chromatography: Results from expeditions between 1977 and 1990, report, 121 pp., Carbon Dioxide Inf. Anal. Cent., Oak Ridge Natl. Lab., Oak Ridge, Tenn., 1992.

S. Carson, A. Gnanadesikan, and J. R. Toggweiler, Geophysical Fluid Dynamics Laboratory, National Oceanic and Atmospheric Administration, P.O. Box 308, Princeton, NJ 08648, USA. (sc@gfdl.noaa.gov; a1g@gfdl.noaa.gov; jrt@gfdl.noaa.gov)

R. J. Murnane, Risk Prediction Initiative, Bermuda Biological Station for Research, Inc., P.O. Box 405, Garrett Park, MD 20896, USA. (rmurnane@abbsr.edu)

J. L. Sarmiento, Atmospheric and Oceanic Sciences Program, Princeton University, P.O. Box CN710, Princeton, NJ 08544-0710, USA. (jls@princeton.edu)